Investigation of Bond in Concrete Structures Strengthened with Near Surface Mounted Carbon Fiber Reinforced Polymer Strips

Tarek Hassan[1] and Sami Rizkalla, F.ASCE[2]

Abstract: Fiber reinforced polymer (FRP) materials are currently produced in different configurations and are widely used for the strengthening and retrofitting of concrete structures and bridges. Recently, considerable research has been directed to characterize the use of FRP bars and strips as near surface mounted reinforcement, primarily for strengthening applications. Nevertheless, in-depth understanding of the bond mechanism is still a challenging issue. This paper presents both experimental and analytical investigations undertaken to evaluate bond characteristics of near surface mounted carbon FRP (CFRP) strips. A total of nine concrete beams, strengthened with near surface mounted CFRP strips were constructed and tested under monotonic static loading. Different embedment lengths were used to evaluate the development length needed for effective use of near surface mounted CFRP strips. A closed-form analytical solution is proposed to predict the interfacial shear stresses. The model is validated by comparing the predicted values with test results as well as nonlinear finite element modeling. A quantitative criterion governing the debonding failure of near surface mounted CFRP strips is established. The influence of various parameters including internal steel reinforcement ratio, concrete compressive strength, and groove width is discussed.

DOI: 10.1061/(ASCE)1090-0268(2003)7:3(248)

CE Database subject headings: Bonding; Concrete structures; Beams; Fiber reinforced polymers; Retrofitting.

Introduction

In recent years, fiber reinforced polymer (FRP) composites have emerged as a potential solution to the problems associated with infrastructures. Resistance to electrochemical corrosion, high strength-to-weight ratio, and versatility of fabrication have made FRP materials attractive to civil engineers. Since 1982, externally bonded FRP sheets/strips have been successfully applied to strengthen concrete structures (Meier 1992). Although externally bonded FRP reinforcement performed extremely well in practice, premature debonding failure was observed and identified by many researchers (Saadatmanesh and Ehsani 1989; Sharif et al. 1994; Arduini et al. 1997). Several details were proposed to avoid this type of failure, which is unacceptable from the point of view of structural safety (Swamy and Mukhopadhyaya 1999).

Use of near surface mounted FRP rods and strips can preclude delamination-type failures, frequently observed by using externally bonded reinforcement. Near surface mounting technique becomes particularly attractive for flexural strengthening in the negative moment regions of slabs and decks, where external reinforcement would be subjected to mechanical and environmental damage and would require protective cover, which could interfere with the presence of floor finishes. Near surface mounted steel bars have been used in Europe since 1947. Asplund (1949) carried out tests on concrete beams reinforced with steel bars and others reinforced with steel bars grouted into diamond-sawed grooves. Test results showed identical behavior for both sets of specimens.

Blaschko and Zilch (1999) carried out bond tests on carbon FRP (CFRP) strips inserted inside grooves. Bond tests were conducted on double shear specimens. Test results showed that strengthening using near surface mounted CFRP strips has a greater anchoring capacity compared to externally bonded CFRP strips. Gentile and Rizkalla (1999) conducted an extensive experimental program to investigate the feasibility of using near surface mounted (GFRP) bars for flexural strengthening of timber bridge stringers. Based on test results, the Tourond Creek bridge constructed 39 years ago in Manitoba, Canada, was strengthened using GFRP bars. The bars were inserted longitudinally in specially constructed grooves in the stringers and adhered to the wood beams with an epoxy resin. Using this technology, the bridge is capable now to carry the current AASHTO design loads for less than 15% of the cost estimated to replace the bridge.

Carolin et al. (2001) tested a series of concrete beams strengthened with near surface mounted CFRP strips. Test results demonstrated the effectiveness of the near surface mounting technique compared to the externally bonded technique. Carolin et al. recommended replacing the epoxy, used in bonding the strips to the surrounding concrete, with cement mortar to improve the work environment on site.

Nordin et al. (2001) conducted a pilot study on concrete beams strengthened with prestressed near surface mounted CFRP strips. Test results showed a substantial increase in cracking and failure loads for the strengthened specimens. Prestressing the strips did not influence the mode of failure. Compared to unstrengthened

[1]Post Doctoral Fellow, Dept. of Civil Engineering, North Carolina State Univ., Campus Box 7533, Raleigh, NC 27695-7533.

[2]Distinguished Professor, Dept. of Civil Engineering, North Carolina State Univ., Campus Box 7533, Raleigh, NC 27695-7533. E-mail: sami_rizkalla@ncsu.edu

Note. Discussion open until January 1, 2004. Separate discussions must be submitted for individual papers. To extend the closing date by one month, a written request must be filed with the ASCE Managing Editor. The manuscript for this paper was submitted for review and possible publication on January 8, 2002; approved on May 3, 2002. This paper is part of the ***Journal of Composites for Construction***, Vol. 7, No. 3, August 1, 2003. ©ASCE, ISSN 1090-0268/2003/3-248–257/$18.00.

J. Compos. Constr., 2003, 7(3): 248-257

specimens, the prestressed beams had considerably smaller deflections at failure.

De Lorenzis and Nanni (2001) investigated the structural performance of simply supported reinforced concrete beams strengthened with near surface mounted GFRP and CFRP rods. Both flexural and shear strengthening were examined. Test results showed that the use of near surface mounted FRP rods is an effective technique to enhance flexural and shear capacity of reinforced concrete beams. The beams strengthened in bending showed an increase in capacity ranging from 26 to 44% over the control beam. For the beams strengthened in shear, an increase in capacity as high as 106% was achieved.

Hassan and Rizkalla (2002) investigated the feasibility of using different strengthening techniques as well as different types of FRP for strengthening concrete structures. Large-scale models of a prestressed concrete bridge were tested to failure. Test results showed that the efficiency of near surface mounted CFRP strips was three times that of the externally bonded strips.

Hassan (2002) proposed a general methodology to evaluate the development length of near surface mounted FRP bars of different configurations and types of fibers. The influence of the groove dimensions, groove spacing, and the limited adhesive cover was investigated. Hassan and Rizkalla concluded that the tensile stresses at the concrete-adhesive interface as well as at the FRP-adhesive interface are highly dependent on the groove dimensions and controls the mode of failure of near surface mounted FRP bars. Design charts were provided to establish code specifications for the use of near surface mounted FRP reinforcement.

Experimental Program

To evaluate the bond characteristics and load transfer mechanism between near surface mounted CFRP strips and concrete, a total of nine simply supported T-beams with a span of 2.5 m and a depth of 300 mm were tested. Shear reinforcement consisted of double-legged 10 M steel stirrups, uniformly spaced at 100 mm. The top flange was reinforced with welded wire fabric 51×51 MW5.6×MW5.6. The top reinforcement consisted of two 10 M steel bars. The bottom reinforcement consisted of two 10 M steel bars running along the full length of the beam and two 15 M steel bars placed at 100 mm from the midspan section of the beam on both sides as shown in Fig. 1. This arrangement of the bottom reinforcement was selected to identify the location of the flexural failure of the strengthened specimens. The T-section configuration was selected to avoid compression failure due to crushing of the concrete. Selection of the specimens' dimensions was finalized after testing six pilot specimens to ensure that rupture of near surface mounted CFRP strips can be achieved if they are bonded along the full length of the beam.

With the maximum moment occurring at the midspan section of the beam, failure could be due to: (1) debonding of the CFRP strips or (2) rupture of the CFRP strips. Specimens were adequately designed to avoid concrete crushing and premature failure due to shear. In case of bond failure, the bond length of the CFRP reinforcement was increased in the subsequent specimens. In case of flexural failure, the bond length was decreased in the following specimens. This scheme was applied until an accurate development length of near surface mounted CFRP strips was achieved.

Strengthening Procedures

One beam was tested as a control specimen while the other eight beams were strengthened with near surface mounted CFRP strips.

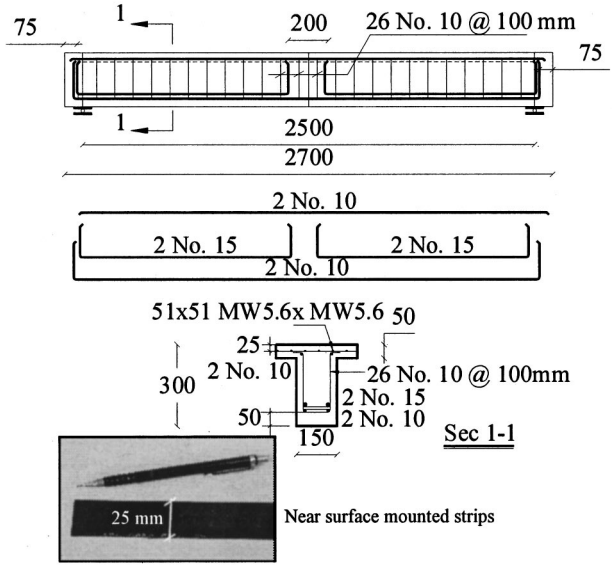

Fig. 1. Reinforcement details of test specimens

Each beam was strengthened using one CFRP strip inserted into a groove cut at the bottom surface of the beam. The strips, as provided by the manufacturer have a nominal width of 50 mm and a total thickness of 1.2 mm. In order to insert the strip within a typical concrete cover used for concrete members, the strips were cut into two halves each, 25 mm wide. Using a concrete saw, approximately 5 mm wide and 25 mm deep grooves were cut into the bottom surface of the beams. The grooves were injected with epoxy adhesive to provide the necessary bond with the surrounding concrete. The strips were carefully placed into the grooves to ensure that they were completely covered with the epoxy. Installation procedures of the strips are illustrated in Fig. 2. Eight different embedment lengths of 150, 250, 500, 750, 850, 950, 1,050, and 1,200 mm were investigated to evaluate the minimum embedment length required to develop the ultimate force of the strip.

The CFRP strips are produced by S&P Clever Reinforcement Company, Switzerland. The strips have a modulus of elasticity of 150 GPa and an ultimate tensile strength of 2,000 MPa as reported by the manufacturer. En-Force CFL epoxy adhesive was used for bonding the strips to the concrete. The epoxy is produced by Structural Composites, Inc., Waller, Tex. The average compressive strength of concrete after 28 days was 48 MPa.

Test Setup and Instrumentation

The beams were tested under a concentrated load applied at midspan. A closed-loop MTS, 1,000 kN testing machine was used to apply the load using stroke control mode. The rate of loading was 1.0 mm/min up to yielding of the internal steel reinforcement, beyond which the rate was increased to 3.0 mm/min up to failure. The instrumentation used to monitor the behavior of the beams during testing is shown in Fig. 3.

Test Results and Discussion

A total of nine concrete beams were tested as given in Table 1. The sequence of testing started first by testing specimens B1, B2, B3, and B4 with embedment lengths of 150, 250, 500, and 750 mm, respectively. Based on the results of these tests, Specimens

J. Compos. Constr., 2003, 7(3): 248-257

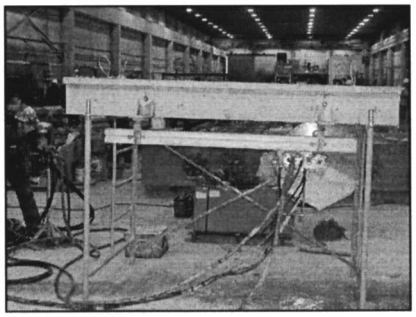

a - Cutting the groove

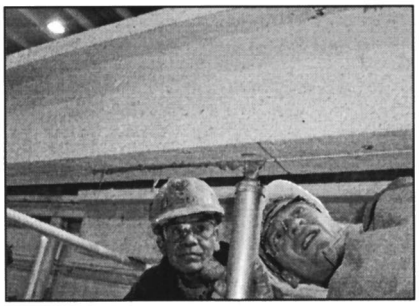

b - Filling the groove with epoxy

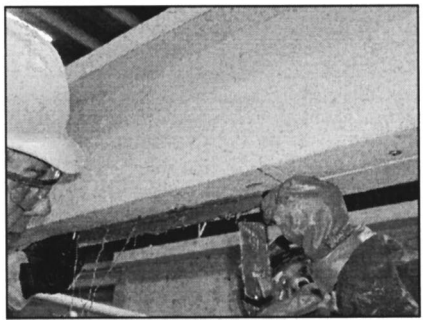

c - Inserting the CFRP Strip inside the groove

Fig. 2. Strengthening procedures

B5 to B8 with embedment lengths ranged from 850 to 1,200 mm were tested. The load-deflection behavior of the control Specimen B0 and the eight strengthened specimens is shown in Fig. 4. The control Specimen B0 failed due to crushing of concrete at a load level of 52 kN. The figure clearly indicates that using embedment lengths up to 250 mm provides insignificant improvement in strength. This is attributed to the early debonding of the CFRP strips.

A considerable enhancement in strength was observed for embedment lengths greater than 250 mm. Specimens B3 and B4 with embedment lengths of 500 and 750 mm, respectively, failed also due to debonding of the CFRP strips. Debonding was observed at both ends of the strips as well as at midspan. This is attributed to shear stress concentration at the cutoff point as well as at the vicinity of flexural cracks. However, final debonding of the CFRP strips was always controlled by the high shear stress at the strips' cutoff points. The failure loads for both beams were 60 and 74 kN, respectively. This indicates that full composite action has not yet been developed and therefore, the measured ultimate load was increasing with the increase of the embedment length. Beams B5, B6, B7, and B8 were strengthened using embedment lengths ranged from 850 to 1,200 mm. The failure of these beams was due to rupture of the CFRP strips as shown in Fig. 5. The maximum measured tensile strain in the CFRP strips used for Specimens B5, B6, B7, and B8 was approximately 1.3%. The measured failure loads for the four beams were almost identical. These results suggest that the minimum embedment length needed to rupture the near surface mounted CFRP strips, with the given dimensions used in this program is 850 mm. Experimental results for the test specimens are summarized in Table 1.

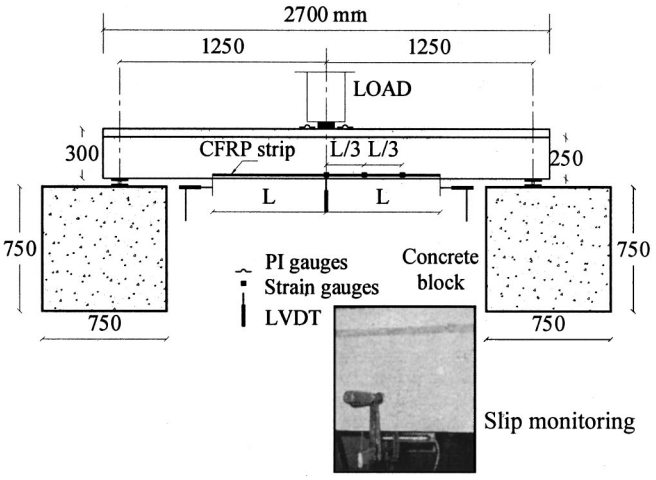

Fig. 3. Instrumentation used for test specimens

Fig. 6 shows the tensile strain in the CFRP strip at ultimate for different embedment lengths used in this study. The measured strain values suggest the following three mechanisms as the embedment length increases: (1) For small embedment lengths (less

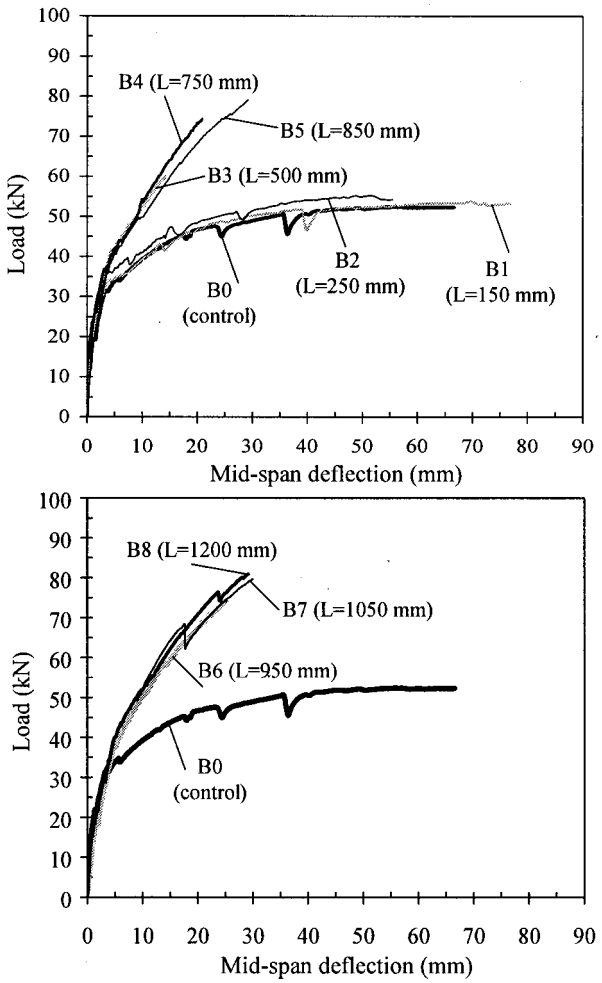

Fig. 4. Load-deflection behavior of test specimens

J. Compos. Constr., 2003, 7(3): 248-257

Table 1. Test Results

Beam no.	Embedment length, L (mm)	Failure load P_u (kN)	Ultimate strain in CFRP (%)	Mode of failure
B0	Control	52	-	C [a]
B1	150	53	0.049	D [b]
B2	250	54	0.17	D
B3	500	60	0.71	D
B4	750	74	1.18	D
B5	850	79	1.27	R [c]
B6	950	75	1.28	R
B7	1050	80	1.29	R
B8	1200	80	1.31	R

[a] Refers to crushing of concrete with steel yielding.
[b] Refers to debonding of the near surface mounted CFRP strip.
[c] Refers to rupture of the near surface mounted CFRP strip.

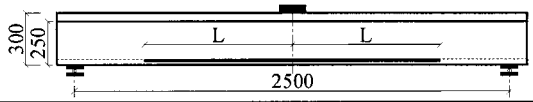

than 250 mm, used for Beams B1 and B2) debonding of the adhesive from the surrounding concrete occurred before yielding of the internal steel reinforcement without significant development of the bond. For these small embedment lengths, the failure is due to immediate debonding, ''destressed mechanism.'' The CFRP strips were completely debonded at a very early stage and the beams' behavior was controlled by the original steel reinforcement as before the application of the strengthening scheme. Linear behavior was observed up to cracking, followed by a nonlinear behavior until yielding of the steel reinforcement took place. After yielding of the steel reinforcement, the increase in the applied load was negligible until crushing of the concrete occurred. No significant improvement in strength or stiffness was achieved; (2) ''bond development mechanism,'' where the strains at failure are increasing linearly with the increase of the embedment length (Beams B3 and B4). For this range of embedment lengths, increasing the bond length results in a considerable enhancement in

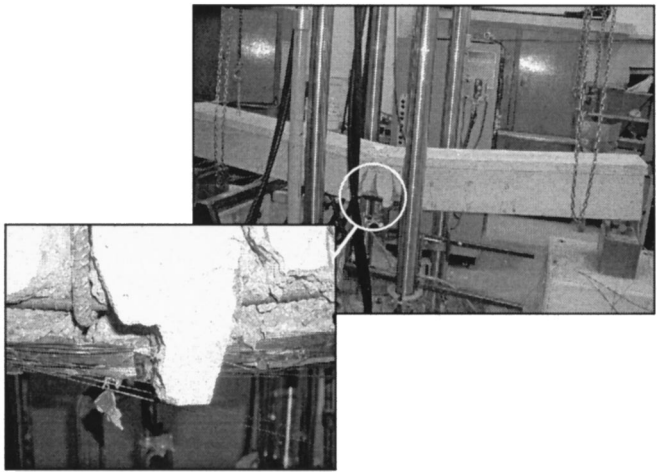

Fig. 5. Rupture of near surface mounted CFRP strips

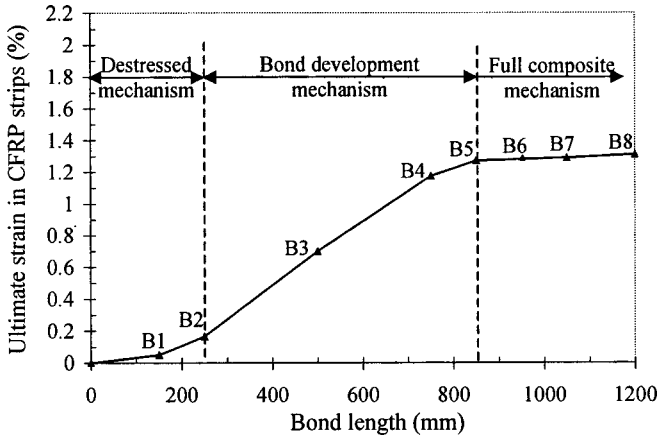

Fig. 6. Maximum tensile strain in CFRP strips at failure versus bond length

the ultimate load carrying capacity of the beams; and (3) ''full composite mechanism,'' where the CFRP behaved in a full composite action with beam. For these relatively long embedment lengths, increasing the embedment length will not provide extra strength to the retrofitted beam (Beams B5, B6, B7, and B8).

Analytical Model

The proposed model is based on the combined shear-bending model introduced by Malek et al. (1998) for externally bonded FRP plates. The model is modified to account for the double bonded area of near surface mounted strips. The model accounts also for the continuous reduction in flexural stiffness due to cracking of the concrete. The derivation of the model is based on the assumption that shear and bending stresses can be investigated separately. Debonding of near surface mounted strips is assumed to occur as a result of high shear stress concentration at cutoff point. The proposed model accounts only for cases where debonding failure is initiated from the strip cutoff points. Other cases where debonding failure is initiated as a result of flexural cracks or at crack intersections are not considered in the proposed approach. Considering the equilibrium of an infinitesimal portion of the strengthened concrete beam, shown in Fig. 7, the shear

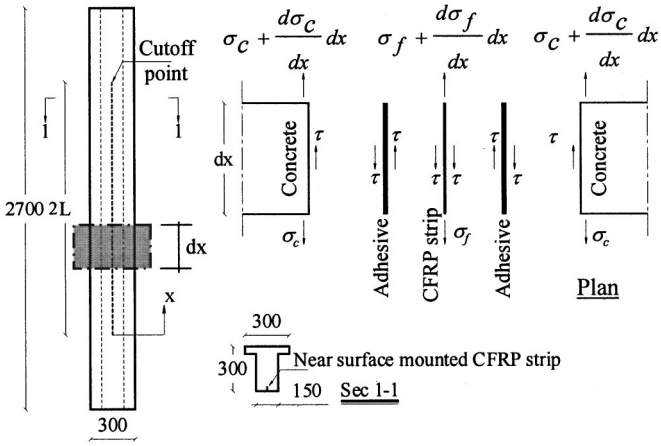

Fig. 7. Infinitesimal portion of test specimen

J. Compos. Constr., 2003, 7(3): 248-257

stress τ along a length of dx can be derived in terms of the incremental normal stress in the CFRP strip $d\sigma_f$ and the thickness of the CFRP strip t_f as follows:

$$\tau = \frac{1}{2}\frac{d\sigma_f}{dx}t_f \tag{1}$$

Assuming linear shear stress-strain relationship for the adhesive

$$\tau = G_a\gamma \tag{2}$$

where G_a and γ=shear modulus and shear strain of the adhesive, respectively.

Assuming linear strain-displacement relationships for the adhesive

$$\gamma = \frac{du}{dz} + \frac{dw}{dx} \tag{3}$$

where u and w=longitudinal and transverse displacements of the adhesive, respectively. Using Eq. (1), and differentiating with respect to x results in

$$\frac{d^2\sigma_f}{dx^2} = \frac{2G_a}{t_f}\left(\frac{d^2u}{dx\,dz} + \frac{d^2w}{dx^2}\right) \tag{4}$$

$d^2u/dxdz$ can be expressed as

$$\frac{d^2u}{dx\,dz} = \frac{d}{dz}\left(\frac{du}{dx}\right) = \frac{d}{dz}(\varepsilon_f - \varepsilon_c) = \frac{1}{t_a}(\varepsilon_f - \varepsilon_c) = \frac{1}{t_a}\left(\frac{\sigma_f}{E_f} - \frac{\sigma_c}{E_c}\right) \tag{5}$$

where ε_f and ε_c=interfacial strain of the CFRP strip and concrete, respectively; E_f and E_c=modulus of elasticity of the CFRP strip and concrete, respectively; t_a=thickness of the adhesive layer; and σ_f and σ_c=normal stress in the CFRP strip and concrete, respectively.

From symmetry

$$\frac{d^2w}{dx^2} = 0 \tag{6}$$

The governing differential equation for the tensile stress in near surface mounted CFRP strips can be expressed as

$$\frac{d^2\sigma_f}{dx^2} - \frac{2G_a}{t_a t_f E_f}\sigma_f = -\frac{2G_a}{t_a t_f E_c}\sigma_c \tag{7}$$

Rewriting Eq. (7)

$$\frac{d^2\sigma_f}{dx^2} - \omega^2\sigma_f = -\omega^2 n\,\sigma_c \tag{8}$$

where

$$\omega^2 = \frac{2G_a}{t_a t_f E_f} \tag{9}$$

$$n = \frac{E_f}{E_c} \tag{10}$$

For simply supported beams subjected to a concentrated load at midspan, the normal stress in concrete σ_c can be evaluated in terms of the effective moment of inertia, I_{eff} as follows:

$$\sigma_c = \frac{Pl_o y_{\text{eff}}}{2I_{\text{eff}}} + \frac{P\,y_{\text{eff}}}{2I_{\text{eff}}}x \tag{11}$$

where P=applied concentrated load; l_o=unbonded length of the CFRP strip; x=longitudinal coordinate starting from cutoff point; and y_{eff}=distance from the CFRP strip to the neutral axis of the section. The above expression is conditioned by the loading configuration and can be easily formulated for other load cases as given in the Appendix. To account for the continuous reduction in flexural stiffness due to cracking of concrete, I_{eff} can be expressed as:

$$I_{\text{eff}} = \left(\frac{M_{\text{cr}}}{M_a}\right)^3 I_{g\ (\text{transformed})} + \left(1 - \left(\frac{M_{\text{cr}}}{M_a}\right)^3\right) I_{\text{cr (transformed)}}$$

[Branson and Trost 1982] (12)

where M_{cr} and M_a=cracking and applied moments on a concrete section, respectively; and I_g and I_{cr}=gross and cracked moment of inertia of the transformed strengthened section, respectively.

The corresponding neutral axis depth can be expressed as

$$c_{\text{eff}} = \left(\frac{M_{\text{cr}}}{M_a}\right)^{2.5} c_g + \left(1 - \left(\frac{M_{\text{cr}}}{M_a}\right)^{2.5}\right) c_{\text{cr}}$$

[Branson and Trost 1982] (13)

where c_g and c_{cr}=neutral axis depth for gross and cracked transformed strengthened sections, respectively.

$$y_{\text{eff}} = d_f - c_{\text{eff}} \tag{14}$$

where d_f=depth of near surface mounted strips from compression fiber.

Rewriting Eq. (8)

$$\frac{d^2\sigma_f}{dx^2} - \omega^2\sigma_f = -\omega^2 n\left(\frac{Pl_o y_{\text{eff}}}{2I_{\text{eff}}} + \frac{Py_{\text{eff}}}{2I_{\text{eff}}}x\right) \tag{15}$$

The general solution for Eq. (15) can be expressed as

$$\sigma_f = C_1 e^{\omega x} + C_2 e^{-\omega x} + \frac{nPy_{\text{eff}}}{2I_{\text{eff}}}x + \frac{nPl_o y_{\text{eff}}}{2\,I_{\text{eff}}} \tag{16}$$

where C_1 and C_2=constants. The solution represents a characteristic solution for σ_f as

$$\sigma_{f_{\text{characteristic}}} = C_1 e^{\omega x} + C_2 e^{-\omega x} \tag{17}$$

and a particular solution for σ_f as

$$\sigma_{f_{\text{particular}}} = \frac{nPy_{\text{eff}}}{2I_{\text{eff}}}x + \frac{nPl_o y_{\text{eff}}}{2I_{\text{eff}}} \tag{18}$$

The shear stress can be expressed as

$$\tau = \frac{t_f}{2}\left[C_1\omega\, e^{\omega x} - C_2\omega\, e^{-\omega x} + \frac{nPy_{\text{eff}}}{2I_{\text{eff}}}\right] \tag{19}$$

Constants C_1 and C_2 can evaluated using the following boundary conditions:

$$\sigma_f = 0 \quad \text{at } x = 0 \tag{20}$$

$$\tau = 0 \quad \text{at } x = L \tag{21}$$

where L=embedment length of the CFRP strip. Using the above boundary conditions, the following expressions for C_1 and C_2 are derived:

$$C_1 = \frac{-n\,Py_{\text{eff}}}{4\,\omega I_{\text{eff}}\cosh(\omega L)}[1 + \omega l_o e^{-\omega L}] \tag{22}$$

$$C_2 = -C_1 - \frac{nPl_o y_{\text{eff}}}{2I_{\text{eff}}} \tag{23}$$

J. Compos. Constr., 2003, 7(3): 248-257

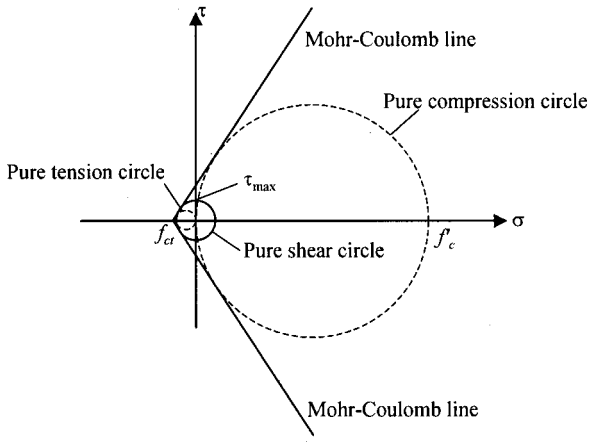

Fig. 8. Mohr-Coulomb failure criterion

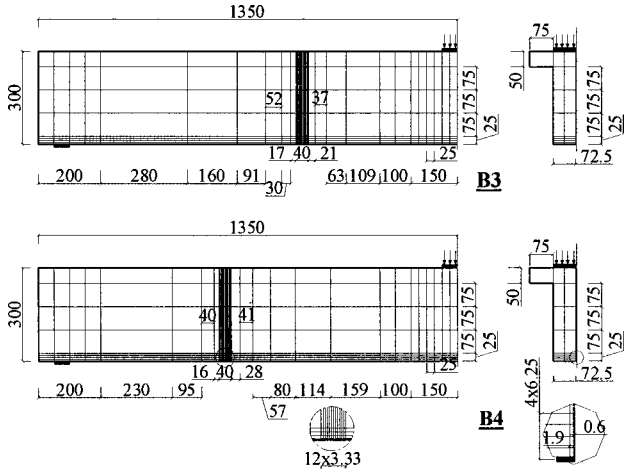

Fig. 9. Mesh dimensions used in finite element analysis

Using practical values for ω and L, $\cosh(\omega L)$ is always a very large number compared to other terms. Therefore, the constant C_1 can be ignored. Rewriting Eq. (19), the shear stress can be expressed as

$$\tau = \frac{t_f}{2}\left[\frac{nPl_o y_{\text{eff}}}{2I_{\text{eff}}}\omega e^{-\omega x} + \frac{nPy_{\text{eff}}}{2I_{\text{eff}}}\right] \tag{24}$$

Debonding will occur when the shear stress reaches a maximum value, which depends on the concrete properties.

Failure Criterion

Many research studies investigated the bond characteristics of FRP strips externally bonded to concrete specimens (Sharif et al. 1994; Quantrill et al. 1996; Arduini et al. 1997). Test results showed that the maximum sustainable interface shear stress ranged between 3.5 to 6 MPa, with failure occurring in the concrete in all cases. Consequently, premature debonding of near surface mounted CFRP strips is governed by the shear strength of the concrete. Other components of the system such as the epoxy adhesive and the CFRP strips have superior strength and adhesion properties compared to concrete. Knowing the compressive and tensile strength of concrete, the Mohr-Coulomb line, which is tangential to both Mohr's circles for pure tension and pure compression, can be represented as shown in Fig. 8. All circles tangential to the Mohr-Coulomb line represent a critical stress combination. The maximum critical shear stress for the pure shear circle is given by

$$\tau_{\max} = \frac{f'_c f_{\text{ct}}}{f'_c + f_{\text{ct}}} \tag{25}$$

where f'_c=compressive strength of concrete after 28 days; and f_{ct}=tensile strength of concrete. Equating the shear strength proposed in Eq. (25) to the shear stress given in Eq. (24), debonding loads for near surface mounted CFRP strips can be determined for this specific loading case and embedment length. Other loading cases are given in the Appendix.

Verification of Analytical Model

The analytical model is verified by comparing the calculated shear stress from Eq. (24) to that obtained from finite element analysis at the cutoff point. The finite element modeling described in this paper was conducted using the *ANACAP* program (Version 2.1). *ANACAP* is known for its advanced nonlinear capabilities of the concrete material model (James 1997). The *ANACAP* software employs the classical incremental theory of plasticity that relates the increment of plastic strain to the state of stresses and stress increment. Formulation of the yield surfaces, loading, and failure surfaces take into account the effect of confinement on the concrete behavior. The concrete material is modeled by the smeared cracking methodology in which progressive cracking is assumed to be distributed over an entire element (Rashid 1968). Verification of the *ANACAP* program using independent experimental results can be found elsewhere (Hassan et al. 2000).

Modeling of Test Specimens

Two test specimens, B3 and B4, were selected from the experimental program to be modeled using finite element analysis. Failure of both beams was due to debonding of the near surface mounted CFRP strips at cutoff points. Taking advantage of the symmetry of the specimens, only a quarter of the beams was modeled. The concrete, epoxy, and the CFRP strip were modeled using 20-node isoparametric brick elements with a $2\times2\times2$ reduced Gauss integration scheme. Each node has three translational degrees of freedom. The load was applied as a uniform pressure acting on an area of 100×150 mm. Several analytical simulations were carried out by varying the size of the elements around the cutoff point. The influence of the mesh size on the predicted shear stresses at cutoff point was noticeable. Mesh dimensions used for Test Specimens B3 and B4 with embedment lengths of 500 and 750 mm, respectively, are shown in Fig. 9. Further refinement of the mesh around cutoff points increased the predicted shear stress by less than 0.5%.

Comparison with Finite Element Analysis

The interfacial shear stress distributions for Specimens B3 and B4 are calculated at two different load levels and compared to those predicted using finite element analysis. The first selected load level was less than the cracking load of the test specimens to validate the analytical model at the elastic stage. The second selected load level matched the cracking load at cutoff points for Specimens B3 and B4. The shear modulus of the epoxy adhesive

J. Compos. Constr., 2003, 7(3): 248-257

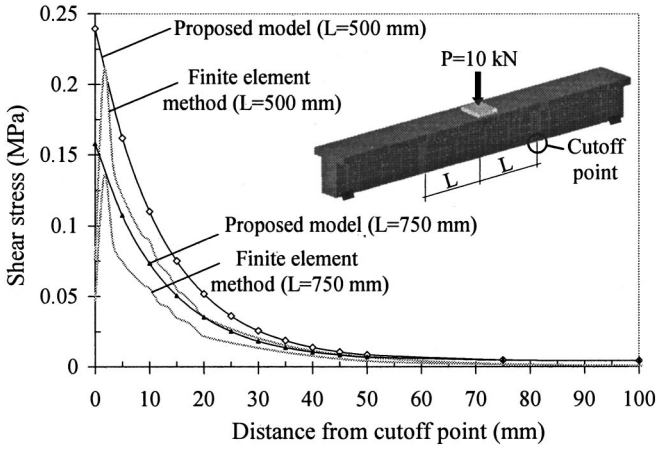

Fig. 10. Comparison of proposed model to finite element method before cracking of concrete at cutoff point

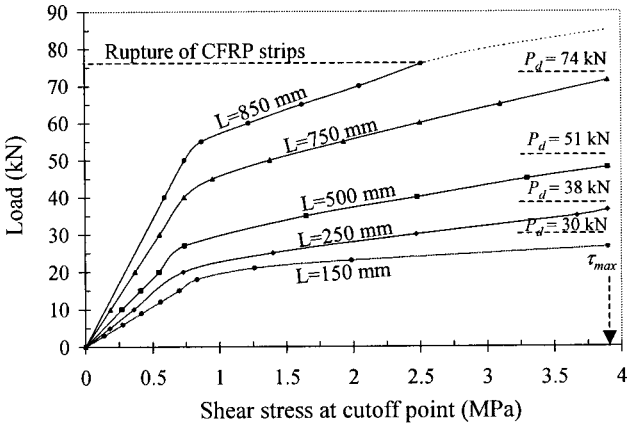

Fig. 12. Maximum shear stress at cutoff point versus applied load

was set to 1,230 MPa as reported by the manufacturer. Based on a groove width of 5 mm, the thickness of the epoxy adhesive used in the analysis was set to 1.9 mm. The results of the finite element analysis together with the proposed analytical model are shown in Fig. 10 at the elastic stage. The results, at the onset of cracking are shown in Fig. 11. Interfacial shear stress distribution, predicted using the analytical model is in a good agreement with the results of the finite element analysis before cracking of the concrete. At the onset of cracking of the concrete at cutoff points, the calculated shear stress distribution is deviated from the finite element results. This behavior is attributed to possible redistribution of shear stresses around the cracks. Such a phenomenon is accounted for in the finite element analysis and not considered in the proposed model. However, the maximum shear stress calculated using the analytical model is in good agreement with the finite element results. Using the proposed model for the effective transformed moment of inertia showed good agreement in predicting the maximum interfacial shear stresses at cutoff points.

Comparison with Experimental Results

Debonding loads are predicted using the proposed analytical model in Eqs. (24) and (25) for different embedment lengths of the CFRP strips as shown in Fig. 12. The measured debonding loads for different embedment lengths are also shown in Fig. 12. In general, the predicted loads at the maximum shear stress for each length are in a good agreement with the measured debonding loads. The predicted debonding loads for Specimens B1, B2, B3, and B4 underestimated the measured values by less than 10%. The proposed model showed good agreement to beams of embedment lengths either at the distressed stage or at the bond development stage. The midspan section of the test specimen was analyzed using a strain compatibility approach to predict the flexural behavior up to failure. The stress-strain relationship of the concrete was modeled using a parabolic relationship in compression. The internal compression force in the concrete was evaluated using the stress-block parameters introduced by Collins and Mitchell (1991). The stress-strain behavior of the CFRP reinforcement was assumed to be linearly elastic up to failure. The average tensile stresses in the concrete between the cracks were considered in the analysis using an average tensile stress-strain relationship for the concrete introduced by Collins and Mitchell (1991). These tensile stresses are concentrated in a zone of concrete around the reinforcement called the ''effective embedment zone'' defined by the CEB-FIP (1978). The tensile stresses in the cracked concrete outside the effective embedment zone are ignored in the analysis. The predicted failure load due to the rupture of the CFRP strip and accounting for the tension stiffening of concrete is 75 kN. Failure of Specimen B5, with an embedment length of 850 mm was due to the rupture of the CFRP strip at a load level of 79 kN, which is 5% higher than the predicted value. Fig. 12 shows also that the minimum embedment length needed to rupture the CFRP strips used in this program is greater than 750 mm and less than 850 mm, which coincides with the experimental results.

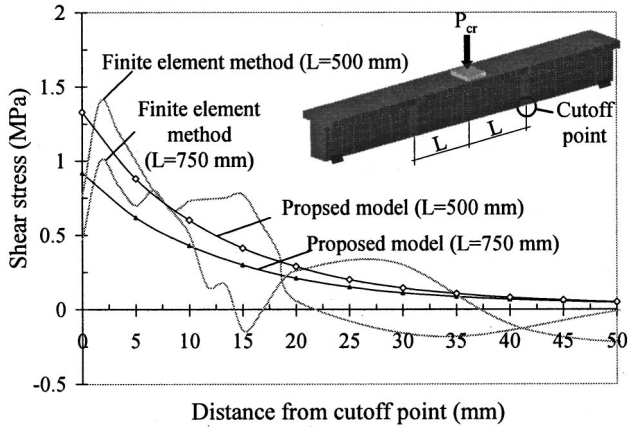

Fig. 11. Comparison of proposed model to finite element method after cracking of concrete at cutoff point

The development length is highly dependent on the dimensions of the strips, concrete properties, adhesive properties, internal steel reinforcement ratio, reinforcement configuration, type of loading, and groove width. The proposed model in Eqs. (24) and (25), can be used to estimate the development length of near surface mounted strips of any configuration as follows:

1. Use the proposed equations, Eqs. (24) and (25), to determine the debonding load of the strip for different embedment lengths as shown in Fig. 13. The resulting curve represents a failure envelope due to debonding of the strip at cutoff point;
2. Use a cracked section analysis at sections of maximum induced normal stresses and determine the ultimate load required to rupture the strip as shown in Fig. 13; and

J. Compos. Constr., 2003, 7(3): 248-257

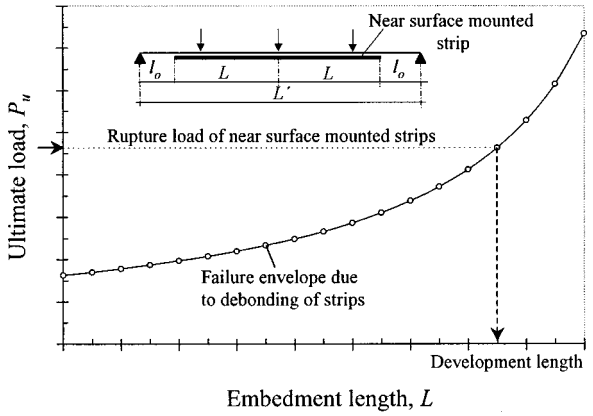

Fig. 13. General procedures to calculate development length of near surface mounted strips

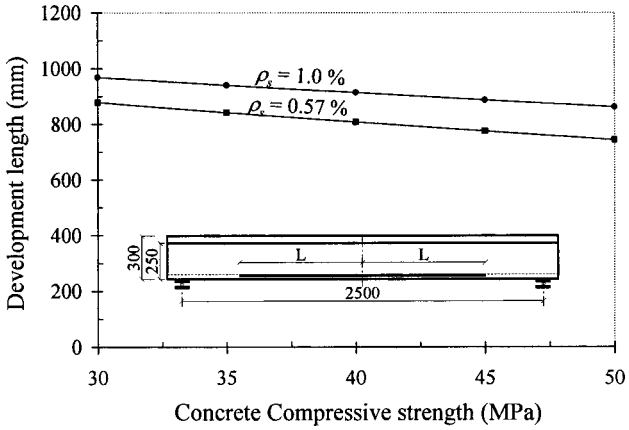

Fig. 15. Influence of concrete compressive strength

3. Determine the development length at the intersection of the line corresponding to flexural failure of the strip with the curve representing debonding failure at cutoff point.

The calculated development length will preclude brittle failure due to debonding of the strips and will ensure full composite action between the strip and concrete up to failure.

Parametric Study

Based on the confidence established in the analytical model, the analysis is extended to investigate the influence of various parameters, believed to affect the development length of near surface mounted CFRP strips. The key parameters are identified as the internal steel reinforcement ratio, concrete compressive strength, and groove width. In the following analysis, tension stiffening of the concrete was not accounted for to simplify the procedure. Fig. 14 shows the influence of the internal steel reinforcement ratio on the development of near surface mounted CFRP strips. Two different sizes of CFRP strips were considered in the analysis. The first strip has a height of 25 mm. The strip can be easily inserted in typical concrete covers. The height of the second strip is 50 mm and was selected to accommodate typical bridge members normally provided with large concrete covers. The thickness of the CFRP strips was set to 1.2 mm in both cases. In general, increasing the internal steel reinforcement ratio shifts down the neutral axis depth and slightly increases the debonding loads. The analysis indicated that failure loads due to the rupture of the CFRP strips were substantially increased with the increase of the reinforcement ratio. Consequently, the development is increased. Such an increase in the development length is highly pronounced at low steel reinforcement ratios. At the absence of the internal steel reinforcement ($\rho_s = 0$), doubling the height of the CFRP strip doubles the failure load due to rupture of the strip. Consequently, the required development length is doubled as shown in Fig. 14. The higher the internal steel reinforcement ratio, the less the contribution of the CFRP reinforcement in increasing the rupture load. Therefore, the influence of doubling the height of the CFRP strip on the development length is significantly reduced for high steel reinforcement ratios as shown in Fig. 14.

The influence of the concrete compressive strength and the groove width is illustrated in Figs. 15 and 16, respectively. The analysis was performed using two different internal steel reinforcement ratios. The first reinforcement ratio was set to 0.57% to match the steel reinforcement ratio at midspan section of the test specimens. The second reinforcement ratio was set to 1% to simulate the most commonly used reinforcement ratio in flexural members. The analysis indicated that failure loads due to the rupture of the CFRP strips were trivially changed with the variation of either the concrete compressive strength or the groove width. However, increasing concrete compressive strength results in a significant increase in the maximum shear stresses τ_{max}. Furthermore, increasing the thickness of the adhesive (by increasing the

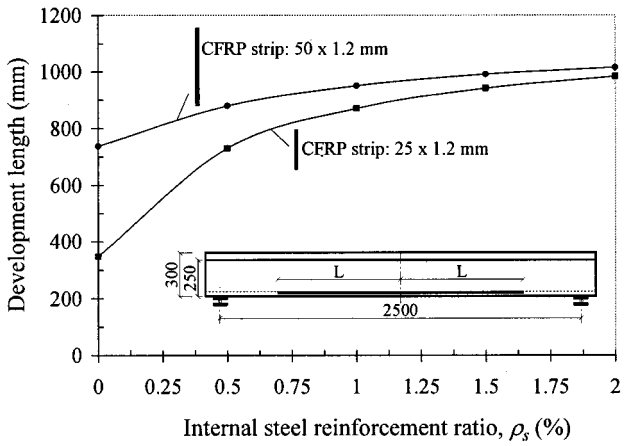

Fig. 14. Influence of internal steel reinforcement ratio

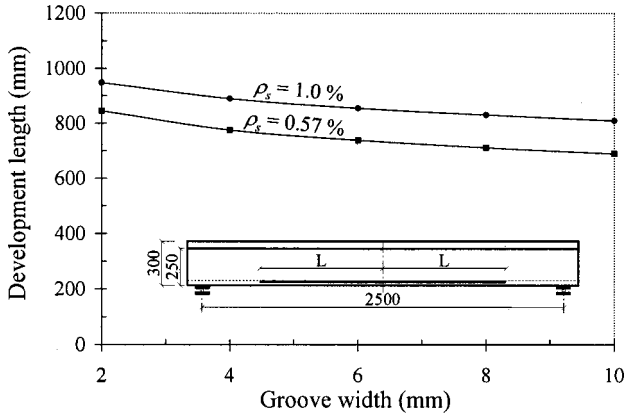

Fig. 16. Influence of groove width

J. Compos. Constr., 2003, 7(3): 248-257

groove width) reduces the shear deformation within the adhesive layer. Consequently, the interfacial shear stresses are reduced. These phenomena result in a significant increase in debonding loads and consequently reduce the development length as shown in Figs. 15 and 16.

Conclusions

Based on the findings of this investigation, the following conclusions can be drawn:

1. The use of near surface mounted CFRP strips is feasible and effective for strengthening/repair of concrete structures;
2. Use of near surface mounted CFRP strips substantially increases both stiffness and strength of concrete beams. The ultimate load carrying capacity of the beams can be increased by as much as 53% for the specimens used in this program. Groove dimensions of 5 mm wide by 25 mm deep were adequate to prevent splitting of the epoxy cover;
3. The proposed analytical model is capable of predicting the interfacial shear stress distribution, ultimate load carrying capacity, and mode of failure of concrete beams strengthened with near surface mounted CFRP strips. Excellent agreement was established between the predicted values using the proposed model and those predicted using finite element analysis;
4. The proposed failure criterion for debonding of near surface mounted CFRP strips provided sufficient evidence and confidence in predicting debonding loads;
5. Debonding loads increase by increasing the embedment length of CFRP strips, concrete compressive strength, and/or groove width;
6. Development length of near surface mounted CFRP strips increases by increasing the internal steel reinforcement ratio. The development length decreases with the increase of either the concrete compressive strength and/or the groove width.

Acknowledgments

The writers wish to acknowledge the support of the Network of Centres of Excellence, ISIS Canada, program of the Government of Canada and the Natural Science and Engineering Research Council. The writers gratefully acknowledge the support provided by S&P Clever Reinforcement Company, Switzerland, Structural Composites Inc., for providing the materials used in the test program. The writers would also like to acknowledge the support provided by Vector Construction Ltd., Winnipeg, Canada for performing all the strengthening work. Special thanks to M. McVey for his assistance during fabrication and testing of the specimens.

Appendix. Shear Stress for Different Loading Configurations

Case I. Simply Supported Beam Subjected to Uniform Load

For a simply supported beam of a span L', subjected to a uniform load q, the induced shear stress τ can be expressed as

$$\tau = \frac{t_f}{2}[ax + b + c\omega e^{-\omega x}] \tag{26}$$

where

$$a = -\frac{qny_{\text{eff}}}{2I_{\text{eff}}} \tag{27}$$

$$b = \frac{qny_{\text{eff}}}{2I_{\text{eff}}}(L' - 2l_o) \tag{28}$$

and

$$c = -\frac{qny_{\text{eff}}}{\omega^2 I_{\text{eff}}} + \frac{qny_{\text{eff}}\, l_o}{2I_{\text{eff}}}(L' - l_o) \tag{29}$$

Case II. Simply Supported Beam Subjected to Two Concentrated Loads

For a simply supported beam subjected to two equal concentrated loads $2P$ placed symmetrically about the center line of the beam, the induced shear stress τ can be expressed as

$$\tau = \frac{t_f}{2}\left[\frac{n\,P\,y_{\text{eff}}}{I_{\text{eff}}} + \frac{nPy_{\text{eff}}l_o}{I_{\text{eff}}}\omega e^{-\omega x}\right] \tag{30}$$

where t_f=thickness of the strip; n=defined by Eq. (10); P=concentrated load; l_o=unbonded length of the strip; ω=defined by Eq. (9); y_{eff}=distance from the strip to the neutral axis of the section; and I_{eff}=effective moment of inertia of the transformed section.

Notation

The following symbols are used in this paper:

C_1, C_2 = parameters in solution of differential equation;
c_{cr} = neutral axis depth for cracked transformed section;
c_{eff} = effective neutral axis depth for transformed section;
c_g = neutral axis depth for gross transformed section;
d_f = depth of near surface mounted CFRP strips from compression fiber;
E_c = modulus of elasticity of concrete;
E_f = modulus of elasticity of CFRP strips;
f'_c = compressive strength of concrete after 28 days;
f_{ct} = tensile strength of concrete;
G_a = shear modulus of adhesive;
h = total height of concrete section;
$I_{\text{cr(transformed)}}$ = cracked moment of inertia of transformed strengthened section;
I_{eff} = effective moment of inertia of transformed strengthened section;
$I_{g(\text{transformed})}$ = gross moment of inertia of transformed strengthened section;
L = embedment length of CFRP strip;
L' = total span of simply supported beam;
l_o = unbonded length of CFRP strip;
M_a = applied moment on concrete section;
M_{cr} = cracking moment of concrete section;
n = defined by Eq. (10);
P = applied concentrated load;
P_{cr} = applied concentrated load that causes cracking at cutoff points;
P_d = experimental debonding load;
P_u = failure load;

J. Compos. Constr., 2003, 7(3): 248-257

q = applied uniform load;
t_a = thickness of adhesive layer;
t_f = thickness of CFRP strip;
u = longitudinal displacement in adhesive layer;
w = transverse displacement in adhesive layer;
x = longitudinal coordinate starting from cutoff point of CFRP strip;
y_{eff} = distance from CFRP strip to neutral axis;
γ = shear strain in adhesive;
ε_c = interfacial strain of concrete;
ε_f = interfacial strain of CFRP strips;
ε_u = strain of near surface mounted CFRP strips at failure;
ρ_s = internal steel reinforcement ratio;
σ_c = normal stress in concrete;
σ_f = normal stress in CFRP strip;
τ = interfacial shear stress;
$\tau_{\max}$ = maximum shear stress at concrete-epoxy interface; and
ω = defined by Eq. (9).

References

Arduini, M., Di Tommaso, A., and Nanni, A. (1997). ''Parametric study of beams with externally bonded FRP reinforcement.'' *ACI Struct. J.*, 94(5), 493–501.

Asplund, S. O. (1949). ''Strengthening bridge slabs with grouted reinforcement.'' *ACI Struct. J.*, 20(4), 397–406.

Blaschko, M., and Zilch, K. (1999). ''Rehabilitation of concrete structures with strips glued into slits.'' *Proc., 12th Int. Conf. on Composite Materials*, Organization of the Int. Conf. on Composite Materials, Paris, CD-ROM.

Branson, D. E., and Trost, H. (1982). ''Unified procedures for predicting the deflection and centrodal axis location of partially cracked nonprestressed and prestressed concrete members.'' *ACI Struct. J.*, 79(2), 119–130.

Carolin, A. Nordin, M. and Taljsten, B. (2001). ''Concrete beams strengthened with near surface mounted reinforcement of CFRP.'' *Proc., Int. Conf. on FRP Composites in Civil Engineering*, Research Centre for Advanced Technology in Structural Engineering, Dept. of Civil and Structural Engineering, The Hong Kong Polytechnic Univ., Hong Kong, 1059–1066.

Comité Euro-International du Béton-Fédération International de la Précontrainte (CEB-FIP). (1978). *Model code for concrete structures: CEB-FIP international recommendations*, 3rd Ed., Comité Euro-International du Béton, Paris, 348 p.

Collins, M., and Mitchell, D. (1991). *Prestressed concrete structures*, Prentice-Hall, Englewood Cliffs, New Jersey.

De Lorenzis, L., and Nanni, A. (2001). ''Shear strengthening of reinforced concrete beams with near-surface mounted fibre reinforced polymer rods.'' *ACI Struct. J.*, 98(1), 60–68.

Gentile, C., and Rizkalla, S. (1999). ''Flexural strengthening of timber beams using FRP.'' *Technical Rep.*, ISIS Canada, Univ. of Manitoba, Winnipeg, Manitoba, Canada.

Hassan, T. (2002). ''Flexural performance and bond characteristics of FRP strengthening techniques for concrete structures.'' PhD thesis, Univ. of Manitoba, Winnipeg, Man., Canada, 304p.

Hassan, T., Abdelrahman, A., Tadros, G., and Rizkalla, S. (2000). ''FRP reinforcing bars for bridge decks.'' *Can. J. Civ. Eng.*, 27(5), 839–849.

Hassan, T., and Rizkalla, S. (2002). ''Flexural strengthening of prestressed bridge slabs with FRP systems.'' *PCI J.*, 47, 76–93.

James, R. G. (1997). *ANACAP concrete analysis program theory manual*, Version 2.1, Anatech Corp., San Diego.

Malek, A., Saadatmanesh, H., and Ehsani, M. (1998). ''Prediction of failure load of R/C beams strengthened with FRP plate due to stress concentration at the plate end.'' *ACI Struct. J.*, 95(1), 142–152.

Meier, U. (1992). ''Carbon fibre-reinforced polymers: Modern materials in bridge engineering.'' *Struct. Eng. Int. (IABSE, Zurich, Switzerland)*, 2, 7–12.

Nordin, H., Taljsten, B., and Carolin, A. (2001). ''Concrete beams strengthened with prestressed near surface mounted reinforcement.'' *Proc., Int. Conf. on FRP Composites in Civil Engineering*, Research Centre for Advanced Technology in Structural Engineering, Dept. of Civil and Structural Engineering, The Hong Kong Polytechnic Univ., Hong Kong, 1067–1075.

Quantrill, R. J., Hollaway, L. C., and Thorne, A. M. (1996). ''Predictions of the maximum plate end stresses of FRP strengthened beams. II.'' *Mag. Concrete Res.*, 48(177), 343–351.

Rashid, Y. R. (1968). ''Analysis of prestressed concrete pressure vessels.'' *Nucl. Eng. Des.*, 7(4), 334–344.

Saadatmanesh, E., and Ehsani, M. R. (1989). ''Application of fibre-composites in civil engineering.'' *Proc., 7th ASCE Structures Congress*, ASCE, New York, 526–535.

Sharif, A., Al-Sulaimani, G. J., Basunbul, I. A., Baluch, M. H., and Ghaleb, B. N. (1994). ''Strengthening of initially loaded reinforced concrete beams using FRP plates.'' *ACI Struct. J.*, 91(2), 160–168.

Swamy, R. N., and Mukhopadhyaya, P. (1999). ''Debonding of carbon fibre reinforced polymer plate from concrete beams.'' *Eng. Structs and Bldgs.*, 134(11), 301–317.